

University of Nebraska - Lincoln

DigitalCommons@University of Nebraska - Lincoln

---

USGS Staff -- Published Research

US Geological Survey

---

3-13-2018

## Irrigated agriculture and future climate change effects on groundwater recharge, northern High Plains aquifer, USA


Zachary H. Lauffenburger

Jason J. Gurdak

Chris Hobza

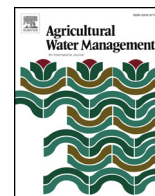
Duane Woodward

Follow this and additional works at: <https://digitalcommons.unl.edu/usgsstaffpub>

 Part of the [Geology Commons](#), [Oceanography and Atmospheric Sciences and Meteorology Commons](#), [Other Earth Sciences Commons](#), and the [Other Environmental Sciences Commons](#)

---

This Article is brought to you for free and open access by the US Geological Survey at DigitalCommons@University of Nebraska - Lincoln. It has been accepted for inclusion in USGS Staff -- Published Research by an authorized administrator of DigitalCommons@University of Nebraska - Lincoln.



# Irrigated agriculture and future climate change effects on groundwater recharge, northern High Plains aquifer, USA



Zachary H. Lauffenburger<sup>a</sup>, Jason J. Gurdak<sup>a,\*</sup>, Chris Hobza<sup>b</sup>, Duane Woodward<sup>c</sup>,  
Cassandra Wolf<sup>a</sup>

<sup>a</sup> San Francisco State University, Department of Earth & Climate Sciences, 1600 Holloway Ave, San Francisco, CA 94132, USA

<sup>b</sup> U.S. Geological Survey, Lincoln, NE 68512, USA

<sup>c</sup> Central Platte Natural Resources District (CPNRD), Grand Island, NE 68803, USA

## ARTICLE INFO

### Keywords:

Groundwater recharge  
Climate change  
Irrigated agriculture  
High plains aquifer  
Diffuse recharge  
Irrigation recharge

## ABSTRACT

Understanding the controls of agriculture and climate change on recharge rates is critically important to develop appropriate sustainable management plans for groundwater resources and coupled irrigated agricultural systems. In this study, several physical (total potential ( $\psi_T$ ) time series) and chemical tracer and dating ( $^3\text{H}$ ,  $\text{Cl}^-$ ,  $\text{Br}^-$ , CFCs,  $\text{SF}_6$ , and  $^3\text{H}/^3\text{He}$ ) methods were used to quantify diffuse recharge rates beneath two rangeland sites and irrigation recharge rates beneath two irrigated corn sites along an east-west (wet-dry) transect of the northern High Plains aquifer, Platte River Basin, central Nebraska. The field-based recharge estimates and historical climate were used to calibrate site-specific Hydrus-1D models, and irrigation requirements were estimated using the Crops Simulation Model (CROPSIM). Future model simulations were driven by an ensemble of 16 global climate models and two global warming scenarios to project a 2050 climate relative to the historical baseline 1990 climate, and simulate changes in precipitation, irrigation, evapotranspiration, and diffuse and irrigation recharge rates. Although results indicate statistical differences between the historical variables at the eastern and western sites and rangeland and irrigated sites, the low warming scenario ( $+1.0^\circ\text{C}$ ) simulations indicate no statistical differences between 2050 and 1990. However, the high warming scenarios ( $+2.4^\circ\text{C}$ ) indicate a 25% and 15% increase in median annual evapotranspiration and irrigation demand, and decreases in future diffuse recharge by 53% and 98% and irrigation recharge by 47% and 29% at the eastern and western sites, respectively. These results indicate an important threshold between the low and high warming scenarios that if exceeded could trigger a significant bidirectional shift in 2050 hydroclimatology and recharge gradients. The bidirectional shift is that future northern High Plains temperatures will resemble present central High Plains temperatures and future recharge rates in the east will resemble present recharge rates in the western part of the northern High Plains aquifer. The reductions in recharge rates could accelerate declining water levels if irrigation demand and other management strategies are not implemented. Findings here have important implications for future management of irrigation practices and to slow groundwater depletion in this important agricultural region.

## 1. Introduction

Accurate estimates of present and future recharge are largely motivated by the need to better manage groundwater resources under current demands and future climate change, particularly for aquifers that currently have unsustainable groundwater abstractions to support irrigated agricultural systems in semiarid and arid regions. Largely in response to the Intergovernmental Panel on Climate Change (IPCC) fourth assessment report (IPCC, 2007) that lacked any substantial mention of groundwater, there has been a growing number of studies to

better understanding how climate variability and change will effect groundwater resources, including recharge (Crosbie et al., 2013; Green et al., 2011; Meixner et al., 2016; Taylor et al., 2013; Treidel et al., 2012). The majority of these studies are either generalized global-level characterization of future recharge trends or basin/location-specific studies (Meixner et al., 2016) that rely on numerical models with varying levels of parametrization from field-based unsaturated hydraulic properties to simulate future recharge rates (Crosbie et al., 2013). There has also been an increasing trend in studies designed to evaluate how the historical conversion of natural rangeland and

\* Corresponding author.

E-mail address: [jgurdak@sfsu.edu](mailto:jgurdak@sfsu.edu) (J.J. Gurdak).

perennial vegetation to irrigated agriculture has influenced recharge rates and mechanisms (Döll, 2009; McMahon et al., 2006; Taylor et al., 2013). However, only two published estimates of future recharge in the western U.S. have considered both climate change and potential changes in farming and irrigation (Meixner et al., 2016). Accurate estimates of historical and future recharge rates under a range of land use/land cover (LULC) and climate change are important for resource managers tasked with developing well-constrained groundwater budgets and conjunctive use strategies with the goal of maintaining sustainable groundwater resources and dependent agroecosystems (Hanson et al., 2012).

Climate variability and change will likely cause significant changes to the spatiotemporal patterns of recharge rates and mechanisms (Crosbie et al., 2013; Green et al., 2011; Meixner et al., 2016). Diffuse recharge that is sourced from precipitation represents about 30% of the world's renewable freshwater resources (Döll, 2009). Irrigation recharge is sourced from irrigation water that infiltrates below the root zone of crops to intercept the water table (Scanlon et al., 2002; McMahon et al., 2006). In addition to diffuse and irrigation recharge, other important recharge mechanisms not included in this study are focused and mountain system recharge (Gurdak et al., 2008; Meixner et al., 2016). The high socioeconomic value of diffuse and irrigation recharge, coupled with concerns about reduced groundwater quality due to nitrate contamination from irrigation recharge (Liao et al., 2012) and the uncertainty surrounding climate variability and change, is driving many management challenges and scientific questions about the current and future recharge and the implications for renewable groundwater resources (Döll, 2009; Green et al., 2011; Taylor et al., 2013; Treidel et al., 2012). Many studies have predicted reduced recharge rates (Crosbie et al., 2013; Earman and Dettinger, 2011; Green et al., 2011; Meixner et al., 2016); however, the effects of climate change might not be negative in all aquifers during the same time period (Döll, 2009; Green et al., 2011; Meixner et al., 2016). The rates and timing of recharge are largely a function of the locally prevailing LULC, hydroclimatologic variables (precipitation, irrigation, evapotranspiration (ET)), and hydraulic properties of the vadose zone. In some regions, irrigation recharge rates beneath irrigated cropland have been reported to be 1–2 or more orders of magnitude greater than diffuse recharge rates beneath adjacent natural rangeland (McMahon et al., 2006; Scanlon et al., 2005, 2006). The vadose zone in semiarid and arid regions can be many tens of meters thick, and have both slowly evolving and dynamic nonlinearities of unsaturated hydraulic properties that pose considerable challenges in efforts to quantify the spatiotemporal pattern of recharge and the temporal lags between LULC and climate change and corresponding recharge dynamics (Corona et al., 2017; Dickinson et al., 2014; Gurdak et al., 2007; Phillips, 1994; Velasco et al., 2017). Additionally, the hydrodynamic responses in the vadose zone to climate variability and changes are not well understood largely because of a general lack of field observations throughout the entire vadose zone and time scales longer than one to two years (Gurdak et al., 2007). Without field observations to calibrate unsaturated flow models and verify model results, approaches such as numerical modeling experiments, sensitivity analyses, and stochastic parameterizations of climate forcings have been used to estimate recharge (Carrera-Hernández et al., 2012; Small, 2005).

The High Plains aquifer in the central U.S. (Fig. 1) is among the most internationally recognized examples of unsustainable groundwater abstractions, which supports one of the largest agricultural economies in the U.S. (Famiglietti, 2014; Gurdak et al., 2012; Konikow, 2015; Scanlon et al., 2005; Taylor et al., 2013). The High Plains aquifer has been studied extensively, with particular emphasis on understanding the controls on recharge along the north-south average annual air temperature gradient (Fig. 1a) (Crosbie et al., 2013; Gurdak et al., 2007; Kuss and Gurdak, 2014; McMahon et al., 2006; Scanlon et al., 2012). Yet, many questions remain about the effects of agricultural LULC, and climate gradients, especially the east-west average annual

precipitation gradient (Fig. 1b), and future climate change on diffuse and irrigation recharge to the High Plains aquifer, particularly at scales consistent with natural resource management (Gurdak et al., 2012; Meixner et al., 2016). Only three published regional-scale studies have estimated future recharge to the High Plains aquifer over the next 50–100 years using model projections (Crosbie et al., 2013; Ng et al., 2010; Rosenberg et al., 1999). To help fill this knowledge gap at the management scale, the U.S. Geological Survey (USGS) established the regional and field-based High Plains Unsaturated-Zone Research Network (HPUZRN) (Fig. 1) to more accurately determine the controls on recharge rates under a range of LULC and across both the north-south air temperature gradient and east-west precipitation gradient (McMahon et al., 2003, 2006, 2007; Gurdak et al., 2007, 2009; Steele et al., 2014). Relying on data from the HPUZRN, this study presents a field- and modeling-based investigation to evaluate the LULC, climatic, and hydrogeologic controls on diffuse and irrigation recharge rates in the northern High Plains aquifer. The specific objectives are as follows. First, field methods are used to quantify irrigation recharge rates beneath two irrigated cropland and diffuse recharge beneath two natural rangeland sites in the USGS HPUZRN along the east-west precipitation gradient in the Platte River Basin of central Nebraska. Second, numerical simulations are used within a probabilistic framework to evaluate the effects of a future 2050 climate relative to a historical 1990 climate on the east-west gradients of precipitation, irrigation demand, ET, and recharge rates at the four study sites. This is the first study of the High Plains aquifer to use field-calibrated unsaturated flow models to simulate historical and future diffuse and irrigation recharge while considering the effects of agricultural LULC, future irrigation demand, and climate change at a spatial scale that is consistent with groundwater management and farming practices.

## 2. Materials and methods

The methods consist of two general components. First, irrigation and diffuse recharge rates were estimated using physical, chemical, and Hydrus-1D (Šimůnek et al., 2008) modeling methods beneath two irrigated cropland and two natural rangeland sites in the USGS HPUZRN within the Central Platte Natural Resource District (CPNRD). Second, the calibrated Hydrus-1D models and climate output from 16 global climate models (GCMs) were used to simulate historical (1990) and future (2050) diffuse recharge rates at the four sites under two carbon dioxide (CO<sub>2</sub>) emission and warming scenarios. Details of the methods are provided next.

### 2.1. Study area

The High Plains aquifer, known locally as the Ogallala aquifer, spans 450,000 km<sup>2</sup> in the Great Plains physiographic province and underlies parts of eight states (Colorado, Kansas, Nebraska, New Mexico, Oklahoma, South Dakota, Texas, and Wyoming) (Fig. 1). The High Plains aquifer is often subdivided because there is little hydraulic connection between the northern, central, and southern High Plains aquifers (McMahon et al., 2007) (Fig. 1). The average depth to groundwater is 15–40 m under natural rangeland and 25–60 m under irrigated cropland (McMahon et al., 2006). Wind-blown silt and sand have created a topography of flat to gentle slopes overlain by coarse-textured soils that allow moderate to high infiltration rates (McMahon et al., 2006). The High Plains region has a middle-latitude dry continental climate and relatively large north-to-south gradients in mean annual air temperature (4–18 °C) and west-to-east gradients in mean annual precipitation (300–840 mm) (Fig. 1).

The High Plains aquifer has the greatest annual groundwater withdrawal of the 62 U.S. principal aquifers (Maupin et al., 2014). Starting in the late 1940s, large-scale irrigation began in the High Plains region (Qi et al., 2002), and by 2000, almost 97% (640 Mm<sup>3</sup> day<sup>-1</sup>) of the total withdrawals (660 Mm<sup>3</sup> day<sup>-1</sup>) were used for irrigation

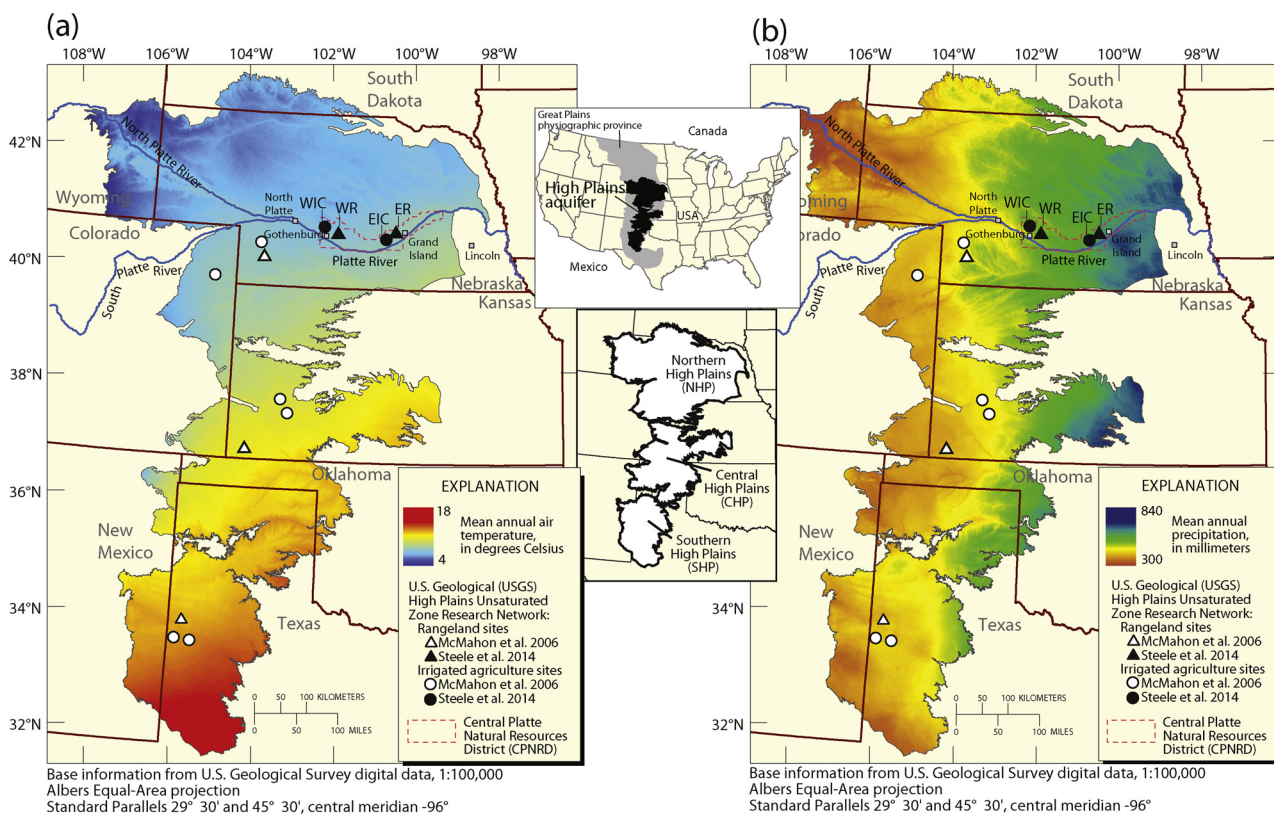


**Fig. 1.** Location of the northern High Plains rangeland and irrigated agricultural study sites on the distribution of regional (a) mean annual air temperature and (b) mean annual precipitation (modified from McMahon et al., 2007). The study includes the eastern rangeland (ER), western rangeland (WR), eastern irrigated corn (EIC), and western irrigated corn (WIC) sites in the Central Platte Natural Resources District (CPNRD). Air temperature and precipitation data credit to Thornton et al., 1997.

(Maupin et al., 2014). The water pumped from the aquifer is used to irrigate crops on about 27% of the irrigated land in the U.S. (Dennehy et al., 2002), and groundwater withdrawals account for about 30% of the Nation’s groundwater used for irrigation (Maupin et al., 2014). Based on 2007 data from the U.S. Department of Agriculture (USDA) National Agricultural Statistics Service, groundwater from the High Plains aquifer supports approximate \$35 billion in crop and food production, which represents approximately 10% of the U.S. total (Scanlon et al., 2012). The large groundwater withdrawals from the High Plains aquifer have resulted in the highest groundwater storage depletion rate of any single aquifer system in the U.S. (Konikow, 2015).

The study area is within the CPNRD in the northern High Plains aquifer (Fig. 1). The CPNRD is mandated by the State of Nebraska to protect groundwater and surface water and other natural resources, and is part of the Platte River Cooperative Hydrology Study (COHYST) that assists the State of Nebraska in meeting the three-state Cooperative Agreement (Luckey and Cannia, 2006).

**2.2. Data acquisition**

Between 2008 and 2010, four vadose zone monitoring sites (Table 1; Fig. 1) were installed in the CPNRD and instrumented following methods outlined by McMahon et al. (2003, 2006) and Gurdak et al. (2007). The study sites were selected as representative locations of long-term diffuse and irrigated recharge across the east-west precipitation gradient of the study area. The eastern rangeland (ER) and eastern irrigated corn (EIC) study sites are southwest of Grand Island, Nebraska, and the western rangeland (WR) and western irrigated corn (WIC) sites are north and northeast of Gothenburg, Nebraska (Table 1; Fig. 1). The four sites are located across the east-west precipitation gradient; historical records show greater average annual precipitation at Grand Island (622 mm yr<sup>-1</sup>, 1962–2009) than at Gothenburg (557 mm yr<sup>-1</sup>, 1895–2010) (NOAA, 2013). The average monthly air temperatures are similar at the four sites; ranging from –5.0 °C in January to 24.9 °C in July (1939–2009) at Grand Island and from –3.7 °C in January to 24.3 °C in July at Gothenburg (1895–2010) (NOAA, 2013). Similar to other sites in the HPUZRN network, the ER, EIC, WR, and WIC sites are designed to evaluate the processes and rates

**Table 1**  
Vadose zone monitoring sites in the Central Platte Natural Resources District Unsaturated-Zone Network (2008–2013) used in this study.

Site	USGS Site ID	Water level bls (m)	Altitude (m)	Latitude	Longitude
eastern rangeland (ER)	410102098374201	20	606.6	41°01'02.5"	–98°37'41.7"
eastern irrigated corn (EIC)	405855098383001	30	618.1	40°58'55.4"	–98°38'30.1"
western rangeland (WR)	405738099504501	15	777.8	40°57'38.3"	–99°50'44.8"
western irrigated corn (WIC)	405855100073901	18	803.1	40°58'54.7"	100°07'38.8"

[Note: bls, below land surface; m, meters; altitude above the North American Vertical Datum of 1988; latitude and longitude North American Datum of 1983; USGS site data available in the USGS National Water Information System (NWIS), <http://waterdata.usgs.gov/nwis>].

of water movement, including diffuse and irrigation recharge rates, and storage and transit times of chemicals in the vadose zone (Gurdak et al., 2009; McMahon et al., 2007). The installation, sample collection and analysis, data, and capabilities of the four sites are provided and detailed by Steele et al. (2014), and summarized below.

At each site a single 15-cm diameter borehole was drilled to the water table using a hollow-stem auger (Steele et al., 2014). During drilling, continuous core samples of the vadose zone were collected using a split-spoon core barrel to collect samples for lithologic descriptions. Each of the approximate 75-cm core lengths from the borehole were cut and divided into five equal subsections for laboratory analysis of physical and chemical properties of the sediment and pore water. One subsection of core was analyzed by the USDA Natural Resources Conservation Service (NRCS) National Soils Survey Laboratory (NSSL) in Lincoln, Nebraska for soil particle-size [L], bulk density ( $\rho_b$ ) [ $M L^{-3}$ ], and water content ( $\theta$ ) [ $L^3 L^{-3}$ ] using the NRCS classification and standard procedures (Soil Survey Staff, 1999). A second subsection of core was analyzed by the USGS Tritium Laboratory in Menlo Park, California, for tritium ( $^3H$ ) in pore water using vacuum distillation; concentrations were quantified by electrolytic enrichment and liquid scintillation counting (Thatcher et al., 1977). The 1-sigma precision of the analysis ranged from 0.3 to 2.8 tritium units (TU) and was lower for moist sediment cuttings than for dry ones (Steele et al., 2014). A third subsection of core was analyzed at the San Francisco State University (SFSU) Groundwater and Water Resources Laboratory for water-extractable concentrations of bromide ( $Br^-$ ), chloride ( $Cl^-$ ), and nitrate ( $NO_3^-$ ) using ion chromatography (Dionex ICS-900 model), with a detection limit of 0.2 micrograms per gram ( $\mu g g^{-1}$ ) and following methods described by Herbel and Spalding (1993), Lindau and Spalding (1984), and McMahon et al. (2003). The remaining two subsections of core were vacuum-sealed, archived at the USGS, and were not used for analysis here.

Heat dissipation probes (HDPs) were installed in the borehole using methods consistent with Gurdak et al. (2007) and McMahon et al. (2006) and at depths of major lithologic units in the vadose zone (Steele et al., 2014). The HDPs measure real-time matric potential ( $\psi_m$ ) values between approximately  $-0.01$  to  $-100$  megapascals (MPa) (Flint et al., 2002), and were programmed to collect  $\psi_m$  measurements at 4-h intervals (Steele et al., 2014). Total water potential ( $\psi_T$ ) values were calculated as the sum of  $\psi_m$  and gravitational potential ( $\psi_g$ ), which assumes that the thermal and osmotic potentials are negligible (Gurdak et al., 2007; McMahon et al., 2006). The borehole was completed with steel surface casing and cement pad to help prevent borehole leakage. Each site was installed with three, vertically-nested monitoring wells with short screens (1.53 m) to determine vertical gradients in groundwater chemistry and age to help estimate recharge rates. The mean screen depths below land surface at each site are ER (24.9, 29.8, and 34.3 m), EIC (51.1, 60.2, and 69.4 m), WR (17.3 and 22.8 m), and WIC (22.1, 26.1, and 29.8 m) (Steele et al., 2014).

A potassium bromide (KBr) solution was evenly applied as a conservative tracer to the land surface within a  $9\text{-m}^2$  area surrounding each of four sites (Steele et al., 2014). Approximately 278 g/L of KBr and de-ionized water mixture was applied evenly to each  $1\text{-m}^2$  grid plot at the ER and EIC sites in May 2009. Approximately 100 g/L of KBr mixture was applied evenly to each  $1\text{-m}^2$  grid plot at the WR and WIC sites in June 2010. Continuous cores were collected at all four sites in April 2012 to determine the infiltration depths of the  $Br^-$  in pore water from the KBr tracer. The water-extractable concentrations of  $Br^-$  in the core were analyzed at the SFSU using ion chromatography methods, as previously described.

### 2.3. Recharge field methods

The physical and chemical data from the four vadose zone monitoring sites were used in a number of field-based methods to evaluate water movement through the vadose zone and to estimate diffuse and

irrigation recharge rates at the sites. Recharge rates were estimated by standard peak-displacement and mass-balance methods for the  $^3H$ ,  $Cl^-$ , and  $Br^-$  tracer data (Allison and Hughes, 1978; Healy, 2010; McMahon et al., 2003) and groundwater-dating methods using atmospheric environmental tracers (chlorofluorocarbons (CFCs-12, -11, and -13), sulfur hexafluoride ( $SF_6$ ),  $^3H$ , and tritium/helium ( $^3H/^3He$ )) (Delin et al., 2000, 2007). HDP time series of  $\psi_T$  ( $\psi_m$  plus  $\psi_g$ ) for selected depths below land surface indicated relatively sharp- and uniform-wetting fronts, similar to  $\psi_T$  profiles seen at the other HPUZRN sites (Gurdak et al., 2007). The HDP  $\psi_T$  profiles were used to verify the wetting fronts simulated by Hydrus-1D. All recharge methods, analytical methods, and data used in the analyses are detailed by Steele et al. (2014), and recharge methods are consistent with the methods used by McMahon et al. (2006) and Gurdak et al. (2007) at the other HPUZRN sites.

### 2.4. Recharge modeling

Four site-specific Hydrus-1D numerical models (Šimůnek et al., 2008) were built to simulate diffuse and irrigation recharge rates under a projected 2050 climate relative to historical climate defined for the year 1990. Hydrus-1D solves Richards' equation (Richards, 1931) for saturated and unsaturated water flow in one-dimension and the advection-dispersion equation for solute transport (Šimůnek et al., 2008). The Hydrus-1D models were calibrated using data from the vadose zone monitoring sites, including soil texture,  $\rho_b$ ,  $\psi_T$ , and  $\theta$ . The historical recharge rates simulated with Hydrus-1D were verified using the field-based recharge estimates.

The Hydrus-1D model domains were bounded at the top by transient atmospheric boundary conditions assuming surface runoff and at the bottom by a zero-gradient boundary condition to simulate freely draining vadose zone profiles. Thus, the water flux across the lower boundary simulates recharge. The transient atmospheric boundary conditions were varied on daily time steps for the following six variables: precipitation, solar radiation, maximum and minimum temperature, relative humidity, and wind speed. The six variables are described in detail in Section 2.5. Hydrus-1D calculates potential ET using the Penman-Monteith combination equation (Monteith, 1981; Monteith and Unsworth, 1990). The vertical length of the model domain for each site was based on site-specific depths to water (Table 1). However, the water table was not included or simulated within the model domain. We used a variable vertical node spacing of 0.03–0.3 m to provide a grid resolution that was finer near the top of the model domain and at interfaces of different soil textures, and coarser near the bottom of the model domain and within each soil texture. The finer node spacing improves the convergence and run-times of the Hydrus-1D models.

The vertical heterogeneities of soil textures in the Hydrus-1D models were based on the results of the previously described USDA NRCS NSSL soil textural analyses of the continuous cores at each site, and corresponding hydraulic properties were defined using the Rosetta Dynamically Linked Library in Hydrus-1D (Schaap et al., 2001). Rosetta uses pedotransfer functions (PTFs) to estimate van Genuchten (1980) water retention parameters and the saturated hydraulic conductivity ( $K_s$ ) in a hierarchical manner from soil textural class information, the soil textural distribution, and  $\rho_b$ , using one or two water retention points as input (Steele et al., 2014).

The Hydrus-1D models simulated root-water uptake using parameters defined by Feddes et al. (1978), with specific values for either pasture (sites ER and WR) or corn (sites EIR and WIR) based on studies by Wesseling et al. (1991). The rangeland (ER and WR) sites are characterized by mixed-grass prairie plant species, including tall and short rhizomatous and bunchgrasses, and many forbs (Kaul and Rolfmeier, 1993). The crop height (2 m) and rooting depth (2.5 m) values for the rangeland Hydrus-1D models (ER and WR) were averaged from root systems of prairie plants (Natura, 1995). The maximum crop height (2 m) and rooting depth (1.7 m) values for the irrigated corn

**Table 2**  
List of 16 global climate models (GCMs) used in this study and abbreviations used in Figures.

Organization	Country	CMIP3 I.D.	Abbreviation
Bjerknes Centre for Climate Research	Norway	BCCR-BCM2.0	BCCR
Canadian Centre for Climate Modelling & Analysis	Canada	CGCM3.1(T63)	CCCMA
Météo-France/Centre National de Recherches Météorologiques	France	CNRM-CM3	CNRM
CSIRO Atmospheric Research	Australia	CSIRO-Mk3.0	CSIRO MK3.0
CSIRO Atmospheric Research	Australia	CSIRO-Mk3.5	CSIRO MK3.5
U.S. Dept. of Commerce/NOAA/Geophysical Fluid Dynamics Laboratory	USA	GFDL-CM2.0	GFDL CM2.0
U.S. Dept. of Commerce/NOAA/Geophysical Fluid Dynamics Laboratory	USA	GFDL-CM2.1	GFDL CM2.1
NASA/Goddard Institute for Space Studies	USA	GISS-ER	GISS
Instituto Nazionale di Geofisica e Vulcanologia	Italy	INGV-SXG	INGV
Institute for Numerical Mathematics	Russia	INM-CM3.0	INMCM
Institut Pierre Simon Laplace	France	IPSL-CM4	IPSL
Center for Climate System Research (The University of Tokyo), National Institute for Environmental Studies, and Frontier Research Center for Global Change (JAMSTEC)	Japan	MIROC3.2(medres)	MIROC
Max Planck Institute for Meteorology	Germany	ECHAM5/MPI-OM	MPI
Meteorological Institute of the University of Bonn, Meteorological Research Institute of KMA, and Model and Data group.	Germany/Korea	ECHO-G	MIUB
Meteorological Research Institute	Japan	MRI-GCGM2.3.2	MRI
National Center for Atmospheric Research	USA	PCM	NCAR

[Note: CMIP3 I.D., Coupled Model Intercomparison Project phase 3 model identification].

Hydrus-1D models (EIR and WIR) were used based on mean maximum plant heights for non-stressed, well-managed crops, and maximum effective rooting depth for common crops outlined in the United Nations Food and Agriculture Organization (FAO) (Allen et al., 1998). Corn stalk and root growth were assumed to be linear over the growing season that extends from late June through early September (Allen et al., 1998).

As an additional Hydrus-1D calibration constraint, a conservative solute was simulated and the resulting solute fluxes and transit depths in the vadose zone were compared to observed fluxes and depths of the applied KBr tracer at each site. The top of each model domain was a concentration flux boundary condition that allowed the initial infiltrating water to simulate a conservative solute concentration similar to the applied KBr tracer concentration. The bottom of each model domain was initially bounded by a zero-concentration gradient.

## 2.5. Historical and future climate data

A 30-year (1981–2011) historical climate data set from the National Oceanic and Atmospheric Administration (NOAA) National Climate Data Center (NCDC) (NOAA, 2013) defined the transient atmospheric boundary conditions in the historical (1990) Hydrus-1D models. The historical climate data were used to calculate saturation vapor pressure (SVP) (kPa) as:

$$SVP = 0.618e^{\frac{17.27 \times T_{avg}}{237.2 + T_{avg}}} \quad (1)$$

where  $T_{avg}$  is average daily temperature ( $^{\circ}\text{C}$ ) (Hendriks, 2010). Relative humidity (RH) (%) was calculated as:

$$RH = \left(1 - \frac{VPD}{SVP}\right) \times 100\% \quad (2)$$

where VPD is vapor pressure deficit (kPa) (Crosbie et al., 2013; Wanielista et al., 1997). Solar radiation data were obtained from the National Center for Atmospheric Research (NCAR)/National Centers for Environmental Prediction (NCEP) (Crosbie et al., 2013; Kalnay et al., 1996). The wind speed data are historical 10-m above vegetation wind speeds obtained from daily  $1/8^{\circ}$  gridded meteorological data (Maurer et al., 2002). Historical wind speed data were used for all historical and future Hydrus-1D models because future wind speed is not simulated by the GCMs.

The 30-year (1981–2011) climate is assumed to be a baseline and representative of historical climate centered around 1990. Using 30 years of historical climate data rather than data from any one particular year minimizes the effects of annual climate variability, and is a method consistent with recent climate-impact studies (Crosbie et al., 2011,

2013). The historical 30-year climate time series was run in Hydrus-1D as a model spin-up to establish the initial conditions of the unsaturated flow models. The spin-up model output data for  $\theta$  and soil temperature at each grid spacing were input into Hydrus-1D as initial profile conditions, and the historical 30-year climate data were re-run to simulate the historical (1990) ET and recharge.

Because the overall objective of the modeling was to investigate the effects on recharge from changes in a projected 2050 climate relative to a 1990 climate, a constant atmospheric  $\text{CO}_2$  concentration was used rather than a time series of  $\text{CO}_2$  concentration. The observed atmospheric  $\text{CO}_2$  concentration in 1990 was 353 ppm (IPCC, 2007), which was assumed to be constant for the historical baseline period. Two future global warming scenarios were used to simulate 2050 conditions: low warming (478 ppm  $\text{CO}_2$  and an increase of  $1.0^{\circ}\text{C}$ ) and high warming (567 ppm  $\text{CO}_2$  and an increase of  $2.4^{\circ}\text{C}$ ). The atmospheric  $\text{CO}_2$  concentrations and associated temperature increases for the low and high warming scenarios were inferred from the IPCC Special Report on Emission Scenarios (SRES) (IPCC, 2007; Nakicenovic and Swart, 2000), and are comparable to the representative concentration pathways (RCPs) for RCP2.6 (increase of  $1.0^{\circ}\text{C}$ ) and RCP8.5 (increase of  $2.0^{\circ}\text{C}$ ) by mid-century (2046–2065) used in the IPCC fifth assessment report (AR5) (IPCC, 2013). A total of 16 different GCMs were used to model each low and high warming scenario (Table 2), thus incorporating as much model uncertainty as possible into the projections (Crosbie et al., 2011; Holman et al., 2011). Daily data for the 16 GCMs were obtained from the World Climate Research Programme's Coupled Model Intercomparison Project phase 3 (CMIP3) multi-model dataset (Crosbie et al., 2013; Meehl et al., 2007).

Following the approach of Crosbie et al. (2012, 2013), the daily scaling method (Chiew et al., 2009) was used to spatially downscale daily time series (precipitation, temperature, VPD, and solar radiation) from the GCM grid scale to the point scale for use in the Hydrus-1D models. Many GCMs indicate that future extreme high precipitation is likely to be more intense, even in some regions where a decrease in mean seasonal or annual precipitation is projected (Chiew et al., 2009). The Chiew et al. (2009) method created future temporal sequencing of precipitation similar to historical precipitation, but scales changes in daily precipitation intensity, as outlined in Crosbie et al. (2013).

Irrigation requirements for corn were estimated from the Nebraska Department of Natural Resources simulations (Bradley et al., 2010) using the Crops Simulation Model (CROPSIM), which is a field scale soil water balance model (Martin et al., 2010). The difference between ET and effective precipitation were plotted against net irrigation for the CROPSIM Grand Island (eastern study area) ( $r^2 = 0.76$ ) and Gothenburg (western study area) ( $r^2 = 0.77$ ) models. The polynomial

**Table 3**

Estimated diffuse recharge rates ( $\text{mm yr}^{-1}$ ) from field-based tritium ( $^3\text{H}$ ), chloride mass-balance (CMB), potassium bromide tracer methods, and groundwater-dating methods (modified from Steele et al. (2014)), and simulated conservative solute (tracer) flux ( $\text{mm yr}^{-1}$ ) from the HYDRUS-1D models.

Methods used to estimate diffuse recharge rates ( $\text{mm yr}^{-1}$ )	western rangeland (WR)	eastern rangeland (ER)	western irrigated corn (WIC)	eastern irrigated corn (EIC)
<b>Tritium (<math>^3\text{H}</math>)</b>				
center of mass	4.0	–	–	80
peak displacement	44	–	–	59
<b>Chloride-mass balance (CMB)</b>				
mean	13	21	–	–
range	1.1–68	1.8–96	–	–
<b>Potassium bromide (KBr) tracer</b>				
center of mass	35	38	65	207
peak displacement	201	9.0	65	172
mean of KBr methods	118	24	65	190
<b>Groundwater-dating</b>				
mean	34	24	224	–
<b>HYDRUS-1D simulated tracer</b>				
center of mass (range)	74–153	89–106	79–129	178–218
peak displacement (range)	100–166	37–109	78–128	180–215

[Note: The range of from the CMB represents variability in chloride flux at the land surface, as described in Steele et al., 2014.].

regression equations for the eastern and western study areas were used to estimate irrigation requirements for the historical and future EIC and WIC Hydrus-1D models. Because the rangeland sites do not receive any irrigation water, simulated irrigation was not applied to the ER or WR Hydrus-1D models.

To statistically test the effects of a projected 2050 climate relative to a 1990 climate, the Wilcoxon signed-rank test was used to determine whether the median difference between paired observations equals zero. The median values are statistically different when the  $p$ -values are less than the alpha ( $\alpha$ ) value of 0.05 (95% confidence level).

### 3. Results

#### 3.1. Field-based estimates of recharge rates

Recharge rates that were estimated from the  $^3\text{H}$ ,  $\text{Cl}^-$  mass-balance (CMB), KBr tracers, apparent groundwater ages from groundwater-dating methods, and simulated conservative tracer from the Hydrus-1D models are shown in Table 3. As expected, site-specific recharge estimates vary somewhat by method (Table 3) because of the inherent uncertainties and range in the spatial ( $< 1$  to  $> 1000 \text{ m}^2$ ) and temporal ( $< 1$  to  $> 1000$  years) support scales for each method, which is explained in Scanlon et al. (2002). In general, the recharge rates estimated from the KBr tracer are greater than those estimated from the  $^3\text{H}$ , CMB, or apparent groundwater ages, because the KBr tracer represents infiltration rates and near-surface fluxes that have responded to transient atmospheric conditions since the KBr was applied in 2009. The recharge estimated from the  $^3\text{H}$ , CMB, and apparent groundwater ages are more representative of water flux and recharge rates at the sites over long-term (decadal) time scales. Recharge rates were not estimated at some sites because of flushing of postbomb  $^3\text{H}$  (sites ER and WIC), uncertainties associated with  $\text{Cl}^-$  concentrations in applied irrigation water (sites WIC and EIC), and (or) the apparent ages are older than the groundwater dating methods used in this study (site EIC) (Table 3) (Steele et al., 2014).

Results indicate that spatial patterns in recharge are controlled primarily by LULC and to a lesser extent by average annual west-east (low to high) precipitation gradients (Table 3). The irrigated recharge

rates are generally greater beneath the irrigated corn sites EIC and WIC ( $59\text{--}224 \text{ mm yr}^{-1}$ ) than the diffuse recharge beneath the rangeland sites ER and WR ( $1.1\text{--}201 \text{ mm yr}^{-1}$ ), which is a spatial pattern consistent with findings from previous recharge studies in the High Plains (McMahon et al., 2006; Scanlon et al., 2005). Irrigation return flow, which is the irrigation water that infiltrates below the root zone, contributes to the greater recharge rates beneath irrigated fields. Differences in recharge rates beneath western and eastern sites are less apparent, in part, because recharge could not be estimated using all methods beneath all sites, as previously discussed. However, the available estimates indicate greater recharge rates beneath eastern sites than western sites for most methods. The CMB method indicates greater recharge rates beneath ER (mean,  $21 \text{ mm yr}^{-1}$ ) than WR (mean,  $13 \text{ mm yr}^{-1}$ ) (Table 3). The KBr method indicates greater recharge rates beneath ER (center of mass,  $38 \text{ mm yr}^{-1}$ ) than WR (center of mass,  $35 \text{ mm yr}^{-1}$ ) and greater recharge rates beneath EIC (center of mass,  $207 \text{ mm yr}^{-1}$ ) than WIC (center of mass,  $65 \text{ mm yr}^{-1}$ ) (Table 3). However, the groundwater-dating method indicates greater recharge rates beneath WR (mean,  $34 \text{ mm yr}^{-1}$ ) than ER (mean,  $24 \text{ mm yr}^{-1}$ ). The groundwater-dating methods inherently integrates recharge over a much larger spatial extent than the vadose-zone based  $^3\text{H}$ , CMB, and KBr tracer estimates of recharge, and thus may not accurately represent site-specific conditions beneath WR and ER. As discussed below, the general west-east increasing trend in recharge rates could be a response to the west-east increasing trend in average annual precipitation, which is also a finding that is consistent with some previous studies (Crosbie et al., 2013; Szilagyi et al., 2011, 2013).

#### 3.2. Modeled estimates of historical recharge rates

The results of simulated historical (1981–2011) precipitation, irrigation, ET, and recharge using output from the 16 GCMs are summarized in Figs. 2a, 3a, 4a and b, and 5a and b, respectively. The median of the 30 years of simulated historical (1990) total annual precipitation in the western and eastern study areas are statistically different ( $p$ -value = 0.016), with greater total annual precipitation in the eastern study areas (Fig. 2a; Appendix Table A.1). Similarly, the median of the 30 years of simulated historical (1990) annual irrigation ( $\text{mm yr}^{-1}$ ) (Fig. 3a; Table A. 2) and annual ET ( $\text{mm yr}^{-1}$ ) in the rangeland sites (Fig. 4a; Table A.3) are statistically different ( $p$ -values =  $< 0.001$  and  $< 0.001$ , respectively) between the western and eastern study areas. The sites in the western study area have substantially greater irrigation (Fig. 3a) and ET (Fig. 4a) than corresponding sites in the eastern study area. Although the median ET values are not statistically different ( $p$ -value = 0.277) between the two irrigated corn sites (WIC and EIC) (Fig. 4b; Table A. 3), the median ET values are statistically different between the paired irrigated and rangeland sites in the western (WIC and WR,  $p$ -value  $< 0.001$ ) and eastern (EIC and ER,  $p$ -value  $< 0.001$ ) study area (Fig. 4a and b; Table A. 3). The median ET is greater at the irrigated corn sites (Fig. 4a and b).

The input of historical precipitation, irrigation, and ET resulted in simulated near-surface water and solute fluxes, and recharge rates that compare reasonably well with the respective KBr tracer and other field-based recharge estimates (Table 3) (Fig. 5a and b). The Hydrus-1D simulated tracer fluxes from the center of mass and peak displacement methods (Table 3) were calculated at three time steps (498, 996 and 1,494 days, not shown in Table 3) to correspond with the approximate time since the application and sampling of the KBr tracer at the sites. In general, the simulated tracer tends to overestimate actual KBr tracer fluxes, except at the EIC and WR sites that respectively match and somewhat underestimate the KBr tracer fluxes. The simulated historical recharge rates (Fig. 5a and b) compare reasonably well with the field-based recharge rates (Table 3). The simulated historical recharge rates are within the range of field-based estimates of recharge rates at the WR, WIC, and EIC sites, but tend to overestimate the field-based estimates at the ER site (Fig. 5a and b). The consistency of the simulated

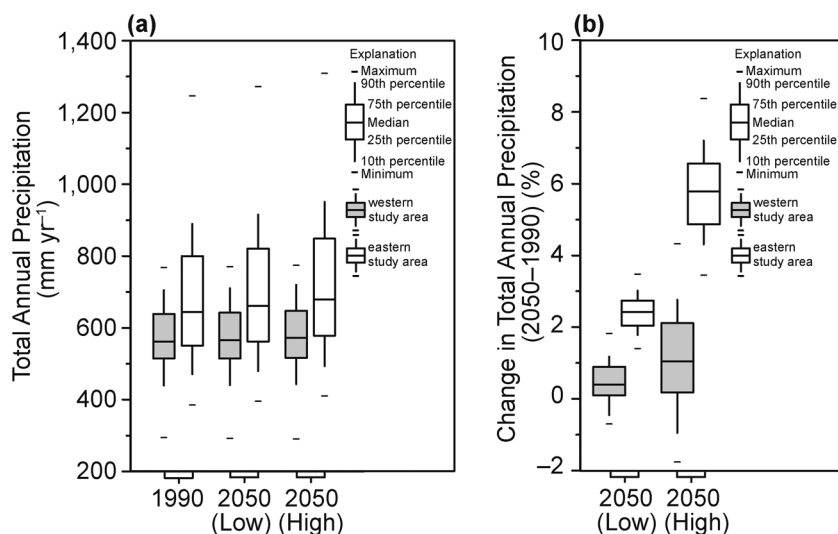


**Fig. 2.** Observed historical (1990) and simulated future (2050) (a) total annual precipitation (mm yr<sup>-1</sup>) and (b) percent (%) change in total annual precipitation at Gothenburg, Nebraska (western study area) and Grand Island, Nebraska (eastern study area) for low (+1.0 °C, 478 ppm CO<sub>2</sub>) and high (+2.4 °C, 567 ppm CO<sub>2</sub>) global warming scenarios. Each boxplot represents the median of 30 years of simulated precipitation from 16 global climate models (GCMs).

near-surface water flux and recharge rates with the field-based near-surface water flux and recharge rates indicates that the Hydrus-1D models have reasonably good predictive ability in estimating historical water fluxes in the near surface and irrigation and diffuse recharge rates.

**3.3. Future climate projections**

Output from the GCMs generally indicates a statistically non-significant increase in average annual precipitation for 2050 relative to 1990 under both the low and high warming scenarios (Fig. 2a; Table A. 1). For the low and high warming scenarios, 50% of the GCMs project an increase in total average annual precipitation for 2050 relative to 1990 at the western study area sites, while 63% project an increase in total average annual precipitation at the eastern study area sites (Appendix Fig. B. 1a and b). However, the median of the 30 years of simulated 2050 relative to 1990 for total annual precipitation in the western and eastern study areas are not statistically different for the low (*p*-values = 0.830, 0.610) or high (*p*-values = 0.739, 0.340) warming scenarios, respectively (Fig. 2a, Table A1). The median for the western study area is projected to have < 1% increase in average annual precipitation relative to historical values for both the low and high global warming scenarios (Fig. 2b). The median for the eastern study area is projected to have a 2.5% and < 6% increase in total average annual precipitation relative to historical values for the low and high

warming scenarios, respectively (Fig. 2b).

Output from the GCMs indicates statistically significant increase in annual irrigation for 2050 relative to 1990 across the study area. For the low global warming scenario, 81% of the GCMs project an increase in annual irrigation at the WIC site, and 88% project an increase at the EIC site (Fig. B. 2b). For the high global warming scenario, 100% of the GCMs project an increase in annual irrigation for the WIC and EIC sites (Fig. B. 2a). Similar to historical irrigation patterns, the projected 2050 relative to 1990 annual irrigation is significantly greater at the WIC than the EIC for the low (*p*-value < 0.001) and high warming (*p*-value < 0.001) scenarios (Fig. 3a, Table A. 2). Under the low warming scenario, there is a projected median increase of approximately 2% and 1% relative to 1990 at the WIC and EIC sites, while under the high warming scenario there is a projected median increase of nearly 15% and 14% relative to 1990 at the WIC and EIC sites, respectively (Fig. 3b).

Output from the GCMs indicates a substantial difference in projected annual ET depending on the warming scenario and LULC. For the low warming scenario, 56% of the GCMs project an increase in average annual ET at the WR site (Figure B. 3c), while only 6% project an increase at the WIC site (Figure B.3d). For the low global warming scenario, 44% of the GCMs project an increase in average annual ET at the ER site (Figure B.3c), and 94% project an increase at the EIC site (Figure B. 3d). For the high global warming scenario, 100% of the 16 GCMs project an increase in average annual ET at all four sites (Figure B.3a

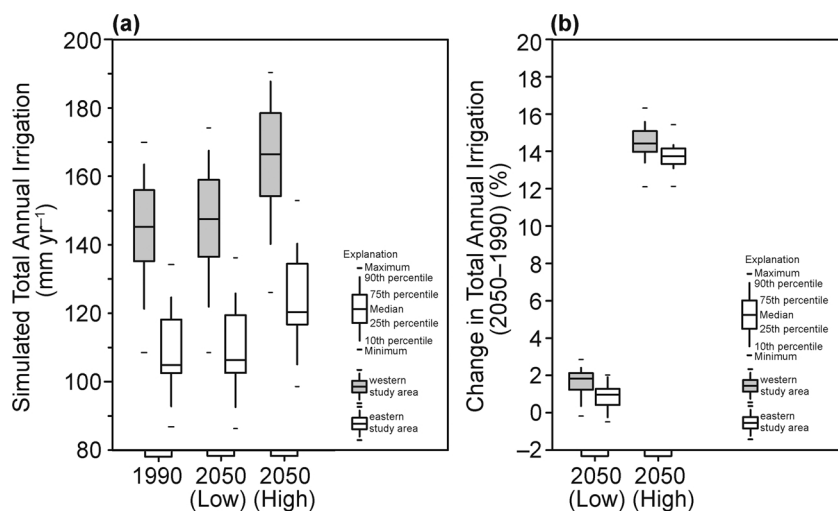


**Fig. 3.** Simulated historical (1990) and future (2050) (a) total annual irrigation (mm yr<sup>-1</sup>) and (b) percent (%) change in total annual irrigation applied at the western (WIC) and eastern irrigated corn (EIC) sites for low (+1.0 °C, 478 ppm CO<sub>2</sub>) and high (+2.4 °C, 567 ppm CO<sub>2</sub>) global warming scenarios. Each boxplot represents the median of 30 years of simulated irrigation based on simulated average annual precipitation and air temperature from 16 global climate models (GCMs).



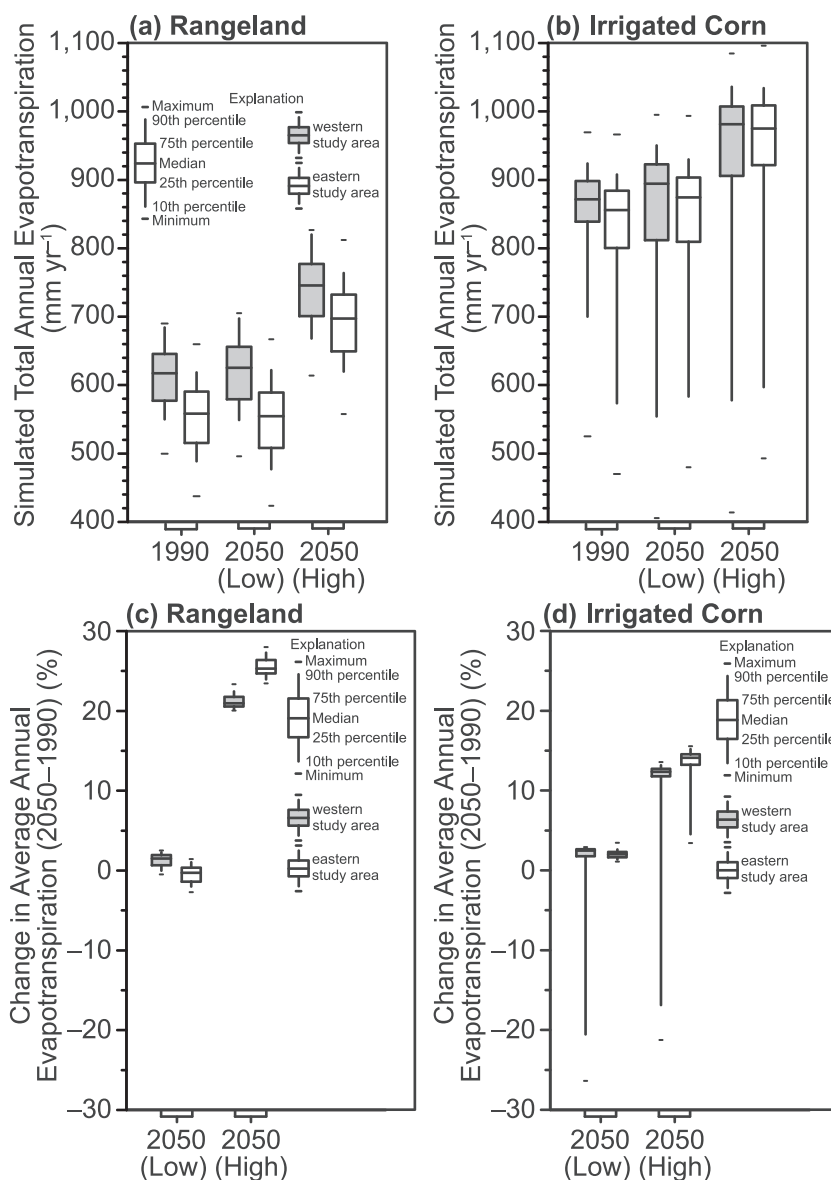


**Fig. 4.** Simulated historical (1990) and future (2050) (a,b) total annual evapotranspiration (mm yr<sup>-1</sup>) and (c,d) percent (%) change in total annual evapotranspiration at the western and eastern study area sites beneath (a,c) rangeland and (b,d) irrigated corn for low (+1.0°C, 478 ppm CO<sub>2</sub>) and high (+2.4°C, 567 ppm CO<sub>2</sub>) global warming scenarios. Each boxplot represents the median of 30 years of simulated average annual evapotranspiration from 16 global climate models (GCMs).

and b). There are no statistical differences in median annual ET between the western ( $p$ -value = 0.412) and eastern ( $p$ -value = 0.877) study sites projected under the low global warming scenario (Fig. 4a and b; Table A. 3). The median annual ET under the low global warming scenario is projected to increase by 2% relative to 1990 values at the WR and WIC sites (Fig. 4c and d), and increase by < 1% at the ER site and about 2% at the EIC site (Fig. 4c and d). However, there are statistical differences in median annual ET between the western ( $p$ -value = < 0.001) and eastern ( $p$ -value = < 0.001) sites projected under the high warming scenario (Fig. 4a and b; Table A. 3). The median annual ET under the high warming scenario is projected to increase by about 21% and 13% relative to 1990 values at the WR and WIC sites, respectively (Fig. 4c and d), and increase by about 25% and 15% at the ER and EIC sites, respectively (Fig. 4c and d).

Output from the GCMs and Hydrus-1D models overwhelmingly indicate decreases in annual recharge for 2050 relative to 1990 across the study area and beneath both types of LULC. For the low warming scenario, 56% of the GCMs project a decrease in average annual recharge

rates at the WR site (Fig. B. 4c), while 100% project a decrease at the WIC site (Fig. B. 4d). For the low warming scenario, 44% of the GCMs project a decrease in average annual recharge rates at the ER site (Fig. B. 4c), and 88% project a decrease at the EIC site (Fig. B. 4d). For the high warming scenario, 94% of the GCMs project a decrease in average annual recharge rates at the WR site (Fig. B. 4a), and 75% project a decrease at the WIC site (Fig. B. 4b). For the high warming scenario, 94% of the GCMs project a decrease in average annual recharge rates at the ER and EIC sites (Fig. B.4a and b). There are no statistical differences in average annual recharge rates between the western ( $p$ -value = 0.0750) or eastern ( $p$ -value = 0.379) study sites projected under the low global warming scenario (Fig. 5a and b; Table A. 4). The median annual recharge for the low global warming scenario is projected to decrease by about 9% and 11% relative to 1990 values at the WR and WIC sites, respectively (Fig. 5c and d), and increase by 6% and decrease by 10% at the ER and EIC sites, respectively (Fig. 5c and d). However, there are statistical differences in median annual recharge rates between the western ( $p$ -value = < 0.001) and eastern ( $p$ -

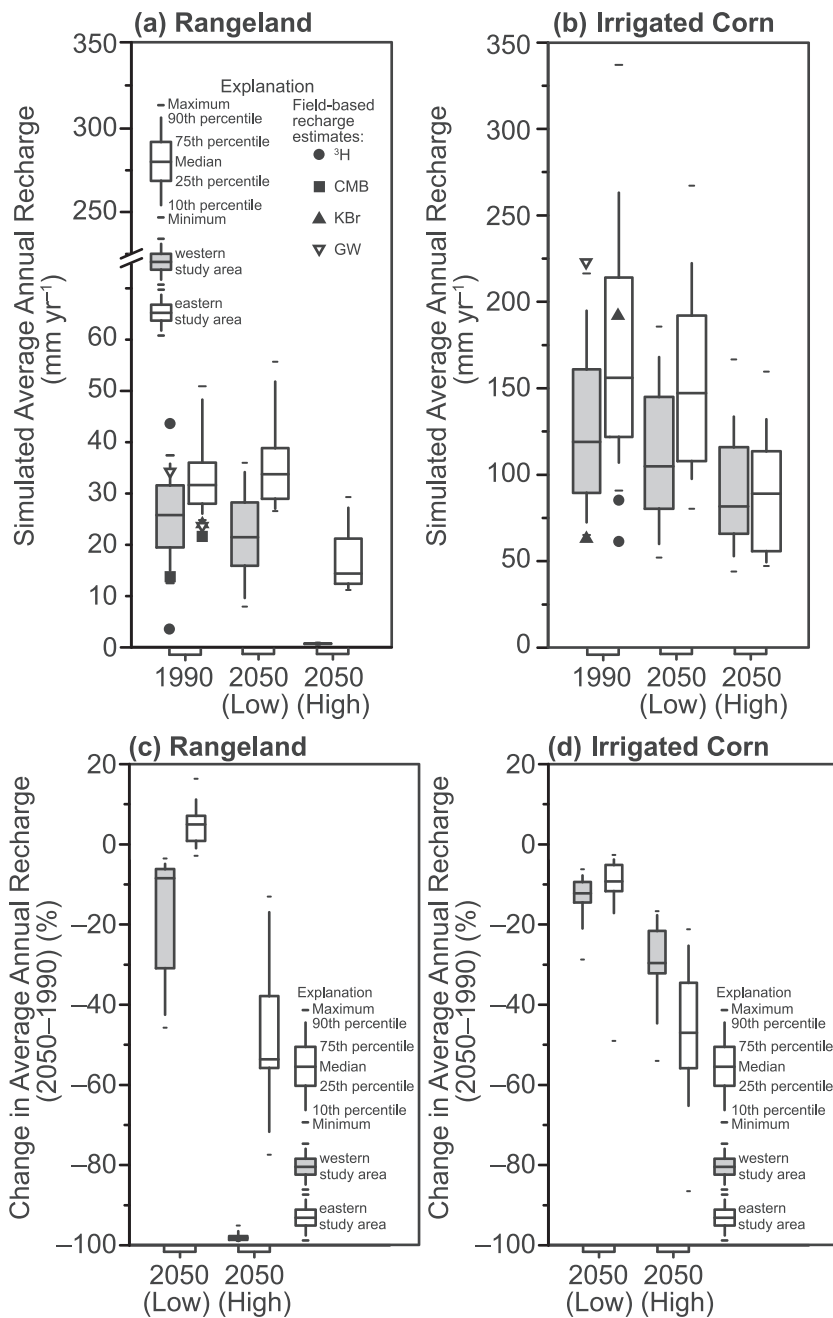


Fig. 5. Simulated historical (1990) and future (2050) (a, c) average annual recharge (mm yr<sup>-1</sup>) and (b,d) percent (%) change in average annual recharge at the western and eastern study area sites beneath (a, c) rangeland and (b, d) irrigated corn for low (+1.0 °C, 478 ppm CO<sub>2</sub>) and high (+2.4 °C, 567 ppm CO<sub>2</sub>) global warming scenarios. Each boxplot represents the median of 30 years of simulated average annual recharge from 16 global climate models (GCMs). The field-based recharge estimates from tritium (3H), chloride-mass balance (CMB), applied potassium bromide tracer (KBr), and groundwater age dating (GW) methods are listed in Table 3.

value = < 0.001) study sites projected under the high global warming scenario (Fig. 5a and b; Table A. 4). The median annual recharge under the high global warming scenario is projected to decrease by about 98% and 29% relative to 1990 values at the WR and WIC sites, respectively (Fig. 5c and d), and decrease by about 53% and 47% at the ER and EIC sites, respectively (Fig. 5c and d).

#### 4. Discussion

The large range of projected precipitation (Figure B. 1), irrigation (Figure B. 2), and ET (Figure B.3) from the 16 GCMs indicates that using output from any single GCM or small group of GCMs to drive hydrologic models such as Hydrus-1D would result in substantial uncertainty in the simulated recharge rates (Figure B. 4). This study characterizes uncertainty by using output from a large number of GCMs to estimate future recharge in a probabilistic framework (Crosbie et al., 2010). Additional uncertainty in the probabilistic framework has been reduced

by calibrating the hydrologic model (Hydrus-1D) with detailed hydraulic data from the vadose zone, and validating the hydrologic model with field-based recharge rates using a range of methods with different spatial and temporal support scales. However, even with a well-calibrated hydrologic model, uncertainty in the output from 16 GCMs translates into a 5% to 70% range in projected recharge under any given LULC, east-west precipitation gradient, or warming scenario (Fig. 5c and d). In this study, diffuse recharge beneath the rangeland is projected to have the least (5%, WR site) and greatest (70%, ER site) range in projected change under the high warming scenario (Fig. 5c). The models tend to agree that the rangeland in the western study area will experience substantial decreases in diffuse recharge, while the models are less consistent in the magnitude of the decrease in diffuse recharge beneath rangeland in the eastern study area under both low and high warming scenarios (Fig. 5a).

The combined output from the probabilistic framework clearly indicates important differences in projected climate and recharge under

the low (+1.0 °C) and high (+2.4 °C) warming scenarios. Under the low warming scenario, the distributions of annual precipitation, irrigation demands, ET, and recharge rates for a projected 2050 future, relative to historical 1990, are not statistically different. However, under the high warming scenario, the distributions of annual precipitation, irrigation demands, ET, and recharge rates for a projected 2050 future, relative to historical 1990, are statistically different. These findings indicate an important threshold or tipping point between +1.0 °C and +2.4 °C warming in the northern High Plains that could trigger significant changes in local irrigation and diffuse recharge.

Findings from this study are generally consistent with the (i) inverse relation between average annual air temperature and historical recharge rates along the regional north-south gradient of the entire High Plains aquifer (McMahon et al., 2006), and the (ii) positive relation between average annual precipitation and historical recharge along the west-east gradient of the northern High Plains (Steele et al., 2014). However, this study demonstrates an important and substantial bidirectional (west to east and south to north) shift in median recharge rates of the northern High Plains aquifer in response to the high warming scenario. First, the projected 2050 air temperature for the northern High Plains is similar to that of present-day central High Plains (Fig. 1), which results in a substantial decrease in recharge rates at all study sites (Fig. 5c and d) that are similar to historical recharge rates for the central High Plains aquifer (McMahon et al., 2006). Second, the projected 2050 recharge rates for the eastern study area are lower than the historical recharge rates for the western study area (Fig. 5a and b), and the projected 2050 recharge rates for the western study area are similar to that of the southern and central High Plains (McMahon et al., 2006). Interestingly, the eastward shift in median recharge rate is less a function of projected changes in precipitation (Fig. 2) and more a function of the projected eastward shift in ET (Fig. 4a and b). Unlike temperature and ET, projected 2050 total annual precipitation is statistically the same as 1990 values for the eastern and western sites (Fig. 2a and b), which highlights the sensitivity of projected recharge to shifting ET regimes.

The probabilistic framework of simulated recharge rates has the additional benefits of helping to communicate findings to groundwater managers that are planning for sustainable development of local groundwater resources in the northern High Plains aquifer. For example, the distribution of future recharge rates (Fig. 5a–d) helps communicate the concept of uncertainty, and enables groundwater managers to select various percentiles (5% and 95%; 10% and 90%, etc.) from the distributions as scenarios in groundwater models and other management planning tools. Regardless of the specific percentiles, groundwater managers of the northern High Plains aquifer must prepare for substantial reductions in future recharge rates beneath rangeland and irrigated corn fields. Higher temperatures and increased ET will alter the timing of demand for irrigation water, as different crops are grown in response to climate change (Karl et al., 2009). Local groundwater managers could consider working with agricultural producers to plant increasingly water-efficient and heat-tolerant crops that should reduce the irrigation demand. The reductions in recharge rates could accelerate declining water levels if irrigation demand and other management strategies are not implemented. Because the bidirectional shift in climate and recharge is regional in nature, groundwater managers could consider development of communication networks and educational opportunities to share and learn from best-management strategies and irrigation practices in neighboring groundwater management districts.

## 5. Conclusions

The 16 GCMs, together with two global warming scenarios, were used to produce 32 projections of future precipitation, ET, and recharge rates for each of the four study sites, and 32 projections of future irrigation demands at the two irrigated corn sites. The low-global-warming

scenario showed no statistical evidence for a change in any future climate variable. However, the high-global-warming scenario showed significant changes, with statistically significant evidence for decreases in average annual recharge rates, and increases in average annual ET and irrigation demands at all four study sites. Precipitation under the high-global-warming scenario did not show statistical evidence for a change from historical median annual values. Median annual irrigation demands increased by as much as 15%, median annual ET increased by as much as 25%, and median annual recharge rates decreased as much as 98%, compared to simulated historical annual averages.

The major finding from this study is the projected bidirectional shift in climate and corresponding recharge rates in the northern High Plains. The north-south temperature gradient is projected to shift north, where future northern High Plains temperatures will resemble current central High Plains temperatures. The east-west recharge rate gradient is projected to shift east, where future recharge rates at the eastern study sites will resemble current recharge rates at the western study sites. Recharge rates under a future climate are particularly sensitive to ET. The east-west ET gradient will shift west, such that future ET at the western study sites will resemble current ET at the eastern study sites. With higher ET and no change in precipitation, future irrigation demand will likely increase, adding further stress on the groundwater resources in the northern High Plains.

## Acknowledgements

Funding for this research was provided by the Nebraska Department of Natural Resources Commission Interrelated Water Management Fund and Water Sustainability Fund, National Science Foundation (NSF) Hydrologic Sciences program (award #EAR-1316553), and the United Nations Educational, Scientific, and Cultural Organization (UNESCO) International Geoscience Program (IGCP) (project # 618). We thank collaborators Drs. Russell Crosbie (CSIRO) and Bridget Scanlon (Bureau of Economic Geology, University of Texas at Austin) for providing the downscaled data from the global circulation models (GCMs) and Greg Steele (retired, U.S. Geological Survey) for assistance with the installation, monitoring, and maintenance of the field sites. Special acknowledgement is given to the land owners that provided access to their land, and to Christopher Green (USGS) and two anonymous reviewers for their comments that improved earlier version of this paper. Any use of trade, firm, or product names is for descriptive purposes only and does not imply endorsement by the U.S. Government.

## Appendix A. Supplementary data

Supplementary data associated with this article can be found, in the online version, at <https://doi.org/10.1016/j.agwat.2018.03.022>.

## References

- Allen, R.G., Pereira, L.S., Raes, Dirk, Smith, Martin, 1998. Crop evapotranspiration—Guidelines for computing crop water requirements: Rome, Food and Agriculture Organization of the United Nations. FAO Drain. Irrig. Paper 56, 300.
- Allison, G.B., Hughes, M.W., 1978. The use of environmental chloride and tritium to estimate total recharge to an unconfined aquifer. *Aust. J. Soil Res.* 16, 181–195.
- Bradley, J., Flyr, B., Gilbert, J., Golt, P., Hallum, D., Kessler, A., Koester, P., Lear, J., Paeglis, L., Pun, M., Schellpeper, J., Schwartzman, K., Vollertsen, R., Wright, A., Zayac, T., Zheng, S., 2010. 2011 Annual Evaluation of Availability of Hydrologically Connected Water Supplies. Nebraska Department of Natural Resources, Lincoln, NE.
- Carrera-Hernández, J.J., Smerdon, B.D., Mendoza, C.A., 2012. Estimating groundwater recharge through unsaturated flow modelling: sensitivity to boundary conditions and vertical discretization. *J. Hydrol.* 452–453, 90–101. <http://dx.doi.org/10.1016/j.jhydrol.2012.05.039>.
- Chiew, F.H.S., Teng, J., Vaze, J., Post, D.A., Perraud, J.M., Kirono, D.G.C., Viney, N.R., 2009. Estimating climate change impact on runoff across southeast Australia: method, results, and implications of the modeling method. *Water Resour. Res.* 45. <http://dx.doi.org/10.1029/2008WR007338>. n/a-n/a.
- Corona, C.R., Gurdak, J.J., Dickinson, J.E., Ferre, T.P.A., Maurer, E.P., 2017. Climate variability and vadose zone controls on damping of transient recharge. *J. Hydrol.* <http://dx.doi.org/10.1016/j.jhydrol.2017.08.028>. <https://www.sciencedirect.com/>

- science/article/pii/S0022169417305607.
- Crosbie, R.S., McCallum, J.L., Walker, G.R., Chiew, F.H.S., 2010. Modelling climate-change impacts on groundwater recharge in the Murray-Darling Basin, Australia. *Hydrogeol. J.* 18, 1639–1656. <http://dx.doi.org/10.1007/s10040-010-0625-x>.
- Crosbie, R.S., Dawes, W.R., Charles, S.P., Mpelasoka, F.S., Aryal, S., Barron, O., Summerell, G.K., 2011. Differences in future recharge estimates due to GCMs, downscaling methods and hydrological models. *Geophys. Res. Lett.* 38. <http://dx.doi.org/10.1029/2011GL047657>. n/a-n/a.
- Crosbie, R.S., Pickett, T., Mpelasoka, F.S., Hodgson, G., Charles, S.P., Barron, O.V., 2012. An assessment of the climate change impacts on groundwater recharge at a continental scale using a probabilistic approach with an ensemble of GCMs. *Clim. Change* 117, 41–53. <http://dx.doi.org/10.1007/s10584-012-0558-6>.
- Crosbie, R.S., Scanlon, B.R., Mpelasoka, F.S., Reedy, R.C., Gates, J.B., Zhang, L., 2013. Potential climate change effects on groundwater recharge in the High Plains Aquifer, USA: climate change effects on recharge in the High Plains. *Water Resour. Res.* 49, 3936–3951. <http://dx.doi.org/10.1002/wrcr.20292>.
- Döll, P., 2009. Vulnerability to the impact of climate change on renewable groundwater resources: a global-scale assessment. *Environ. Res. Lett.* 4, 035006. <http://dx.doi.org/10.1088/1748-9326/4/3/035006>.
- Delin, G.N., Healy, R.W., Landon, M.K., Boehlke, J.K., 2000. Effects of topography and soil properties on recharge at two sites in an agricultural field. *J. Am. Water Resour. Assoc.* 36, 1401–1416. <http://dx.doi.org/10.1111/j.1752-1688.2000.tb05735.x>.
- Delin, G.N., Healy, R.W., Lorenz, D.L., Nimmo, J.R., 2007. Comparison of local- to regional-scale estimates of ground-water recharge in Minnesota, USA. *J. Hydrol.* 334, 231–249. <http://dx.doi.org/10.1016/j.jhydrol.2006.10.010>.
- Dennehy, K.F., Litke, D.W., McMahon, P.B., 2002. The high plains aquifer, USA: groundwater development and sustainability. In: Hiscock, K.M., Rivett, M.O., Davidson, R. (Eds.), *Sustainable Groundwater Development*, Geological Society of London. Geological Society Publishing House, London UK, pp. 99–119.
- Dickinson, J.E., Ferre, T.P.A., Bakker, M., Crompton, B., 2014. A screening tool for delineating subregions of steady recharge within groundwater models. *Vadose Zone J.* 13 (6) vzj2013.10.0184.
- Earman, S., Dettinger, M., 2011. Potential impacts of climate change on groundwater resources—a global review. *J. Water Clim. Change* 2, 213. <http://dx.doi.org/10.2166/wcc.2011.034>.
- Famiglietti, J.S., 2014. The global groundwater crisis. *Nat. Clim. Change* 4, 945–948. <http://dx.doi.org/10.1038/nclimate2425>.
- Feddes, R.A., Kowalik, P., Zaradny, H., 1978. *Simulation of Field Water Use and Crop Yield*. John Wiley & Sons, New York, NY.
- Flint, A.L., Campbell, G., Ellet, K., Calissendorff, C., 2002. Calibration and temperature correction of heat dissipation matrix potential sensors. *Soil Sci. Soc. Am. J.* 66, 1439–1445.
- Green, T.R., Taniguchi, M., Kooi, H., Gurdak, J.J., Allen, D.M., Hiscock, K.M., Treidel, H., Aureli, A., 2011. Beneath the surface of global change: impacts of climate change on groundwater. *J. Hydrol.* 405, 532–560. <http://dx.doi.org/10.1016/j.jhydrol.2011.05.002>.
- Gurdak, J.J., Hanson, R.T., McMahon, P.B., Bruce, B.W., McCray, J.E., Thyne, G.D., Reedy, R.C., 2007. Climate variability controls on unsaturated water and chemical movement, High Plains aquifer, USA. *Vadose Zone J.* 6, 533 10.2136/vzj2006.0087.
- Gurdak, J.J., Walvoord, M.A., McMahon, P.B., 2008. Susceptibility to enhanced chemical migration from depression-focused preferential flow, High Plains aquifer. *Vadose Zone J.* 7 (4), 1218–1230. <http://dx.doi.org/10.2136/vzj2007.0145>.
- Gurdak, J.J., McMahon, P.B., Dennehy, K.F., Qi, S.L., 2009. *Water Quality in the High Plains Aquifer* (No. Circular 1337). U.S. Geological Survey.
- Gurdak, J.J., McMahon, P.B., Bruce, B.W., 2012. Vulnerability of groundwater quality to human activity and climate change and variability, High Plains aquifer, USA. In: Treidel, H., Martin-Bordes, J.L., Gurdak, J.J. (Eds.), *Climate Change Effects on Groundwater Resources: A Global Synthesis of Findings and Recommendations*, International Association of Hydrogeologists, International Contributions to Hydrogeology. Taylor & Francis Publishing, pp. 145–167.
- Hanson, R.T., Flint, L.E., Flint, A.L., Dettinger, M.D., Faunt, C.C., Cayan, D., Schmid, W., 2012. A method for physically based model analysis of conjunctive use in response to potential climate changes. *Water Resour. Res.* 48. <http://dx.doi.org/10.1029/2011WR010774>.
- Healy, R.W., 2010. *Estimating Groundwater Recharge*. Cambridge University Press, Cambridge, UK.
- Hendriks, M.R., 2010. *Introduction to Physical Hydrology*. Oxford University Press, New York, NY.
- Herbel, M.J., Spalding, R.F., 1993. Vadose zone fertilizer derived nitrate and  $\delta^{15}N$  extracts. *Ground Water* 31, 376–382.
- Holman, I.P., Allen, D.M., Cuthbert, M.O., Goderniaux, P., 2011. Towards best practice for assessing the impacts of climate change on groundwater. *Hydrogeol. J.* 20, 1–4. <http://dx.doi.org/10.1007/s10040-011-0805-3>.
- IPCC, 2007. *Climate Change 2007: The Physical Science Basis* (Contribution of Working Group I to the Fourth Assessment Report of the Intergovernmental Panel on Climate Change). Cambridge University Press, Cambridge, U.K.
- IPCC, 2013. In: Stocker, T.F., Qin, D., Plattner, G.-K., Tignor, M., Allen, S.K., Boschung, J., Nauels, A., Xia, Y., Bex, V., Midgley, P.M. (Eds.), *Climate Change 2013: The Physical Science Basis*. Contribution of Working Group I to the Fifth Assessment Report of the Intergovernmental Panel on Climate Change. Cambridge University Press Cambridge, United Kingdom and New York, NY, USA 1535 pp.
- Kalnay, E., Kanamitsu, M., Kistler, R., 1996. The NCEP/NCAR 40-year reanalysis project. *Bull. Am. Meteorol. Soc.* 77, 437–471.
- Karl, T.R., Melillo, J.M., Peterson, T.C., 2009. *Global Climate Change Impacts in the United States: A State of Knowledge Report*. Cambridge University Press, Cambridge, U.K.
- Kaul, R., Rolfsmeier, S., 1993. *Native Vegetation of Nebraska*. University of Nebraska, Lincoln Conservation and Survey Division.
- Konikow, L.F., 2015. Long-term groundwater depletion in the United States. *Groundwater* 53, 2–9. <http://dx.doi.org/10.1111/gwat.12306>.
- Kuss, A.J.M., Gurdak, J.J., 2014. Groundwater level response in U.S. principal aquifers to ENSO, NAO, PDO, and AMO. *J. Hydrol.* 519, 1939–1952. <http://dx.doi.org/10.1016/j.jhydrol.2014.09.069>.
- Liao, L., Green, C.T., Bekins, B.A., Böhlke, J.K., 2012. Factors controlling nitrate fluxes in groundwater in agricultural areas. *Water Resour. Res.* 48 (6). <http://dx.doi.org/10.1029/2011WR011008>.
- Lindau, C.W., Spalding, R.F., 1984. Major procedural discrepancies in soil extracted nitrate levels and nitrogen isotope values. *Ground Water* 22, 273–278.
- Luckey, R.R., Canna, J.C., 2006. *Groundwater Flow Model of the Western Model Unit of the Nebraska Cooperative Hydrology Study (COHYST) Area* (Cooperative Hydrology Study Technical Report). Nebraska Cooperative Hydrology Study.
- Martin, D.L., Supalla, R.J., Thompson, C.L., McMullen, B.P., Hergert, G.W., Burgener, P.A., 2010. *Advances in Deficit Irrigation Management*. Presented at the 5th National Decennial Irrigation Conference. American Society of Agricultural and Biological Engineers, Phoenix, AZ.
- Maupin, M.A., Kenny, J.F., Hutson, S.S., Lovelace, J.K., Barber, N.L., Linsey, K.S., 2010. *Estimated Use of Water in the United States in 2014*. U.S. Geological Survey Circular 1405. <http://dx.doi.org/10.3133/cir1405>. 56 p.
- Maurer, E.P., Wood, A.W., Adam, J.C., Lettenmaier, D.P., Nijssen, B., 2002. A long-term hydrologically based dataset of land surface fluxes and states for the conterminous United States. *J. Clim.* 15, 3237–3251.
- McMahon, P.B., Dennehy, K.F., Michel, R.L., Sophocleous, M.A., Ellet, K., Hurlbut, D.B., 2003. *Water Movement Through Thick Unsaturated Zones Overlying the Central High Plains Aquifer, Southwestern Kansas, 2000–2001* (Water-Resources Investigations Report No. 03-4171). U. S. Geological Survey.
- McMahon, P.B., Dennehy, K.F., Bruce, B.W., Böhlke, J.K., Michel, R.L., Gurdak, J.J., Hurlbut, D.B., 2006. Storage and transit time of chemicals in thick unsaturated zones under rangeland and irrigated cropland, High Plains, United States. *Water Resour. Res.* 42. <http://dx.doi.org/10.1029/2005WR004417>.
- McMahon, P.B., Dennehy, K.F., Bruce, B.W., Gurdak, J.J., Qi, S.L., 2007. *Water-quality Assessment of the High Plains Aquifer, 1999–2004* (Professional Paper No. 1749). U. S. Geological Survey.
- Meehl, G.A., Covey, C., Delworth, T., Latif, M., McAvaney, B., Mitchell, J.F.B., Stouffer, R.J., Taylor, K.E., 2007. The WCRP CMIP3 multimodel dataset: a new era in climate change research. *Bull. Am. Meteorol. Soc.* 88, 1383–1394. <http://dx.doi.org/10.1175/BAMS-88-9-1383>.
- Meixner, T., Manning, A.H., Stonestrom, D.A., Allen, D.M., Ajami, H., Blasch, K.W., Brookfield, A.E., Castro, C.L., Clark, J.F., Gochis, D.J., Flint, A.L., Neff, K.L., Niraula, R., Rodell, M., Scanlon, B.R., Singha, K., Walvoord, M.A., 2016. Impactions of projected climate change for groundwater recharge in the western United States. *J. Hydrol.* 534, 124–138. <http://dx.doi.org/10.1016/j.jhydrol.2015.12.027>.
- Monteith, J.L., Unsworth, M.H., 1990. *Principles of Environmental Physics*, 2nd ed. Edward Arnold, London, UK.
- Monteith, J.L., 1981. Evaporation and surface temperature. *Q. J. R. Meteorol. Soc.* 107, 1–27.
- NOAA, 2013. *National Climatic Data Center, Annual Data, United States, January 2013*. National Oceanic and Atmospheric Administration.
- Nakicenovic, N., Swart, R., 2000. *Emission Scenarios, IPCC Special Reports*. Cambridge University Press, Cambridge, U.K.
- Natura, H., 1995. *Root Systems of Prairie Plants*. Conservation Research Institute, Cedarburg, WI.
- Ng, G.-H.C., McLaughlin, D., Entekhabi, D., Scanlon, B.R., 2010. Probabilistic analysis of the effects of climate change on groundwater recharge. *Water Resour. Res.* 46, W07502. <http://dx.doi.org/10.1029/2009WR007904>.
- Phillips, F.M., 1994. Environmental tracers for water movement in desert soils of the American Southwest. *Soil Sci. Soc. Am. J.* 58, 15–24.
- Qi, S.L., Konduris, A., Litke, D.W., Dupree, J., 2002. *Classification of Irrigated Land Using Satellite Imagery, the High Plains Aquifer, Nominal Date 1992* (Water-Resources Investigations Report No. 2002–4236). U. S. Geological Survey.
- Richards, L., 1931. Capillary conduction of liquids in porous mediums. *Physics* 1, 318–333.
- Rosenberg, N.J., Epstein, D.J., Wang, D., Vail, L., Srinivasan, R., Arnold, J.G., 1999. Possible impacts of global warming on the hydrology of the Ogallala Aquifer region. *Clim. Change* 42, 677–692.
- Scanlon, B.R., Healy, R.W., Cook, P.G., 2002. Choosing appropriate techniques for quantifying groundwater recharge. *Hydrogeol. J.* 10, 18–39.
- Scanlon, B.R., Reedy, R.C., Stonestrom, D.A., Prudic, D.E., Dennehy, K.F., 2005. Impact of land use and land cover change on groundwater recharge and quality in the southwestern US. *Glob. Change Biol.* 11, 1577–1593. <http://dx.doi.org/10.1111/j.1365-2486.2005.01026.x>.
- Scanlon, B.R., Keese, K.E., Flint, A.L., Flint, L.E., Gaye, C.B., Edmunds, W.M., Simmers, I., 2006. Global synthesis of groundwater recharge in semiarid and arid regions. *Hydrol. Process.* 20, 3335–3370. <http://dx.doi.org/10.1002/hyp.6335>.
- Scanlon, B.R., Faunt, C.C., Longuevergne, L., Reedy, R.C., Alley, W.M., McGuire, V.L., McMahon, P.B., 2012. Groundwater depletion and sustainability of irrigation in the US High Plains and Central Valley. *Proc. Natl. Acad. Sci. U. S. A.* 109, 9320–9325. <http://dx.doi.org/10.1073/pnas.1200311109>.
- Schaap, M.G., Leij, F.J., van Genuchten, M.T., 2001. ROSETTA: a computer program for estimating soil hydraulic parameters with hierarchical pedotransfer functions. *J. Hydrol.* 251, 163–179.
- Šimůnek, J., van Genuchten, M.T., Sejna, M., 2008. Development and applications of the HYDRUS and STANMOD software packages and related codes. *Vadose Zone J.* 7,

- 587–600. <http://dx.doi.org/10.2136/vzj2007.0077>.
- Small, E.E., 2005. Climatic controls on diffuse groundwater recharge in semiarid environments of the southwestern United States. *Water Resour. Res.* 41. <http://dx.doi.org/10.1029/2004WR003193>. n/a-n/a.
- Soil Survey Staff, 1999. *Soil Taxonomy – a Basic System of Soil Classification for Making and Interpreting Soil Surveys (Handbook 436)*. Natural Resources Conservation Services, U.S. Department of Agriculture.
- Steele, G.V., Gurdak, J.J., Hobza, C.M., 2014. *Water Movement Through the Unsaturated Zone of the High Plains Aquifer in the Central Platte Natural Resources District, Nebraska, 2008–12 (Scientific Investigations Report 2014–5008)*. U. S. Geological Survey.
- Szilagyi, J., Zlotnik, V.A., Gates, J.B., Jozsa, J., 2011. Mapping mean annual groundwater recharge in the Nebraska Sand Hills, USA. *Hydrogeol. J.* 19, 1503–1513. <http://dx.doi.org/10.1007/s10040-011-0769-3>.
- Szilagyi, J., Zlotnik, V.A., Jozsa, J., 2013. Net recharge vs. depth to groundwater relationship in the platte river valley of Nebraska, United States. *Groundwater* 51, 945–951. <http://dx.doi.org/10.1111/gwat.12007>.
- Taylor, R.G., Scanlon, B., Döll, P., Rodell, M., van Beek, R., Wada, Y., Longuevergne, L., Leblanc, M., Famiglietti, J.S., Edmunds, M., Konikow, L., Green, T.R., Chen, J., Taniguchi, M., Bierkens, M.F.P., MacDonald, A., Fan, Y., Maxwell, R.M., Yecheili, Y., Gurdak, J.J., Allen, D.M., Shamsudduha, M., Hiscock, K., Yeh, P.J.-F., Holman, I., Treidel, H., 2013. Ground water and climate change. *Nat. Clim. Change* 3, 322–329. <http://dx.doi.org/10.1038/nclimate1744>.
- Thatcher, L., Janzer, V., Edwards, K., 1977. *Method for Determination of Radioactive Substances in Water and Fluvial Sediment (Water-Resources Investigations Report No. Book 5, Chapter A5)*. U. S. Geological Survey.
- Thornton, P.E., Running, S.W., White, M.A., 1997. Generating surfaces of daily meteorological variables over large regions of complex terrain. *J. Hydrol.* 190, 214–251.
- Treidel, H., Martin-Bordes, J.L., Gurdak, J.J. (Eds.), 2012. *Climate Change Effects on Groundwater Resources: A Global Synthesis of Findings and Recommendations*. CRC Press, Taylor & Francis Group, London, UK.
- van Genuchten, M.T., 1980. A closed form equation for predicting the hydraulic conductivity of unsaturated soils. *Soil Sci. Soc. Am. J.* 44, 892–898.
- Velasco, E.M., Gurdak, J.J., Dickinson, J.E., Ferre, T.P.A., Corona, C.R., 2017. Interannual to multidecadal climate forcings on groundwater resources of the U.S. West Coast. *J. Hydrol.* 11, 250–265. <http://dx.doi.org/10.1016/j.ejrh.2015.11.018>.
- Wanielista, M.P., Kersten, R., Eaglin, R., 1997. *Hydrology: Water Quantity and Quality Control*, second ed. John Wiley & Sons, New York, NY.
- Wesseling, J., Elbers, J., Kabat, P., van der Broek, B., 1991. *SWATRE: instructions for input*. Winand Star. Cent. Wageningen. Neth. 29.